Chalcogenide Letters Vol. 20, No. 7, July 2023, p. 477 - 485

Fabrication and investigation of zinc telluride thin films

R. H. Athab, B. H. Hussein*
Department of physics, College of Education for Pure Science / Ibn Al-Haitham, University of Baghdad, Baghdad, Iraq

Zinc Telluride ZnTe alloys and thin film have been fabricated and deposited on glass substrates by thermal evaporation method which may be a suitable window layer of zinc telluride with different annealing temperatures (373 and473) K for 60 minutes in vacuum. Deposited thin films with thickness 100 nm was characteristic by using X-ray diffraction XRD to know structures, Atomic Force Microscopy (AFM) to evaluate surface topology, morphology. It was found out that the vacuum annealing improves on thin ZnTe films structure and surface morphology. Structural analysis reveals that ZnTe films have zinc blende structure of cubic phase with (111) preferred reflection and grain size is enhanced from 8.6 to 16.7 nm with annealing. Optical properties where optical bandgap energy values slightly decreased (2.3-2.2) eV as the annealing temperatures.

(Received March 11, 2023; Accepted July 13, 2023)

Keywords: Vacuum annealing, Optical properties, ZnTe, AFM, Thin film

1. Introduction

Zinc telluride (ZnTe) is a member of the II-VI compound semiconductor family including zinc selenide (ZnSe), zinc telluride (ZnTe) , cadmium telluride (CdTe) and cadmium selenide (CdSe) have recognized important attention owing to their low-cost however high absorption coefficients in their uses to a variety of solid state device [1,2]. ZnTe material has brick-red color and the direct bandgap change in the range (2.10-2.26) eV [3,4]. Need to new nanostructured material with better properties. Due to appearances obtained at the deposition method such as: in the visible spectrum high transparency, low resistivity [5,6] ZnTe are sensitive materials in the (green spectral region) [5] with wide energy band-gap (2.26) eV [7,8] low electronic affinity (3.53) eV [5] nanostructured ZnTe films are widely used in various fields such as laser diodes, photodetectors, light emitting diodes, gas sensors, field emission and solar cells [9]. ZnTe can be used as window materials multi-layer solar cell [8] the crystal structure is Cubic structure chalcopyrite with the lattice constant a = 6.101 Å [10]. it can be used as a p-type [8,5]. ZnTe has been deposited by several methods such as rf magnetron sputtering [5,11] glancing angle technique [12] thermal evaporation [7,13,14] electrodeposition [8,15] pulsed laser [16] (MBE)molecular beam epitaxy [17,18] , hot-wall evaporations [19], electron beam evaporation [20,21], chemical spray pyrolysis [22], Multiple Potential Steps [23] high vacuum resistive system[24] chemical bath deposition[25].

This work concentrate for on fabrication of ZnTe by vacuum evaporation technique with thickness 100 nm and study the effect of heat-treated (373,473) K on structures, topology, morphology properties, Optical and Hall effect measurement.

2. Experimental

Thermal evaporation is an easy method for deposition ZnTe thin film 100 nm thickness from alloy of ZnTe, it's been prepared in this work, the high purity (99.999 %) of Zinc (Zn) and telluride (Te) elements stoichiometric proportions by weight (1:1) binary compound ZnTe, after that mix Zinc and telluride elements in evacuated fused quartz ampoules, heated at (1573 K) for six hours, according phase diagram of ZnTe [26,27]. Thin film as deposited by thermal

* Corresponding author: bushrahhz@yahoo.com
https://doi.org/10.15251/CL.2023.207.477

evaporation with the help of diffusion and rotary pumps, the pressure of the chamber was lowered down to 6×10^{-5} mbar by using (E 306), the space between the evaporation (molybdenum boat) and the substrates were 18 cm, then annealing temperatures with vacuum (373 & 473) K. To grow a uniform thin film semiconductor with good adherence to the glass substrate surface, must be thoroughly cleaned to remove any pollution. Scherer's Formula used to determine the crystalline size of the thin film [28], calculated Microstrain (Ɛ) and dislocations density (δ) for fabricated thin films of the ZnTe films from X-ray diffraction [29]. AFM have characterized the morphology of the ZnTe film. Tauc equation and lambert law have been used to calculated the absorption coefficient α and the energy gap (Egopt) respectively from absorption spectrum [30]. Optical Constant such as n: refractive index, k : extinction coefficient, real part ε_r & imaginary part ε_i of dielectric constant can be measured, dielectric loss and optical conductivity [30,31,32]. The carrier type, concentrations and their mobility were measured by Hall effect studies using the Van der Pauw -Ecopia HMS -3000.

3. Results and discussion

The XRD spectrum of the ZnTe films show in Figure (1) with a thickness (100nm) have been studied at (R.T) and heat-treated at (373,473) K for 1 hour. XRD patterns were obtained with wavelength, λ=1.542 Å in the range of 2θ=(20-80)°. All thin films have polycrystalline with cubic crystal structure and three peaks, the preferred orientation was found to be along (111) plane for main peak observed at 25.25 degrees that confirms the nano-crystalline nature of film. Two other peaks with lower intensities (220) & (311) planes of ZnTe observed at 41.8 & 49.49 degrees. all the peaks of diffraction coincide with the reported standard values ICDD 00-015-0746 for ZnTe with cubic crystal phase as shown in Figure (1). We can observe when heat-treated with temperature (373 and 473) K, Intensities peaks increase and grown of C.S where The 2θ position of dominant (111) orientation is slightly swung towards upper 2θ with heat-treated as in [6].

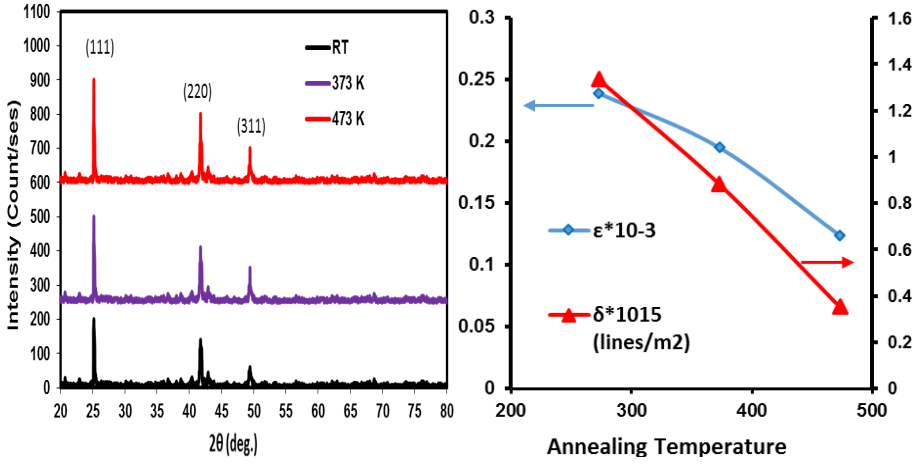

Fig. 1. X-ray diffraction pattern for as deposited ZnTe films and annealed.

The crystallites size is listed in Table (1) estimated by Scherer's formula where it shows that the ZnTe at 473 K have high C.S from other thin film, the decreases in FWHM of major peak which result increases in C.S from 8.6 to 16.73 this result agrees with [6]. As the annealing temperature increases to 373 and 473 K, there is a decrease in both microstrain and dislocation density. This is because the microstrain is directly proportional to the full width at half maximum (FWHM) of the main peak, while the dislocation density is inversely proportional to the size of the crystallites. The decrease in defects within the ZnTe thin films as a result of the annealing process suggests an improvement in their crystal structure and vacuum thermal annealing methods

improve the crystallites size and stoichiometric composition of thin film beside with the decrease in the defects, which could action as carrier trap [33].

Table 1. Experimental XRD data for as deposited and annealed ZnTe films thin.

T_a (K)	d_{exp} (Å)	d_{stand} (Å)	$2\theta_{exp}$ (deg.)	hkl	FWHM (deg.)	C.S (nm)	**$\delta*10^{15}$ (lines/m^2)**	**$\varepsilon*10^{-3}$**
R.T	3.521720	3.523000	25.2587	100	0.98330	8.648532117	1.336	0.2398772
	2.158215	2.159000	41.8047	220				
	1.839331	1.840000	49.4963	311				
373	3.521679	3.523000	25.259	100	0.799840	10.63225353	0.884	0.1951219
	2.158215	2.159000	41.8047	220				
	1.839331	1.840000	49.4963	311				
473	3.521542	3.523000	25.26	100	0.50830	16.73047734	0.352	0.12400040
	2.158215	2.159000	41.8047	220				
	1.839331	1.840000	49.4963	311				

To enhance the analysis of the growth of surface roughness, three-dimensional (3D) AFM can be employed, image and Granularity Cumulation Distribution chart of ZnTe films obtained at R.T and heat-treated at (373,473) K are shown in Figure 2. The average roughness of a surface is determined by the variation in peaks and valleys, and any significant changes in roughness usually indicate a deviation in the development process. it is experiential increased with heat-treated from (1.88 to 3.11 nm). Root mean Sq extra sensitive from the roughness The amount of surface roughness that is most commonly reported is typically associated with significant deviations from the mean plan. Table 2 enlists the physical attributes of the structure that were measured, including the average grain size (G.S), roughness, and root mean square, average grain size varied from (37.70 to 74.44 nm) These observations agree with XRD results.

Table 2. Displays the average surfaces roughness, grain size, and root mean square for as deposited and annealed ZnTe films thin.

Thickness (100nm)	Grain Size (nm)	Surfaces roughness (nm)	Root mean Sq. (nm)
R.T	34.70	1.88	2.49
373	41.32	2.42	3.06
473	74.44	3.11	4.13

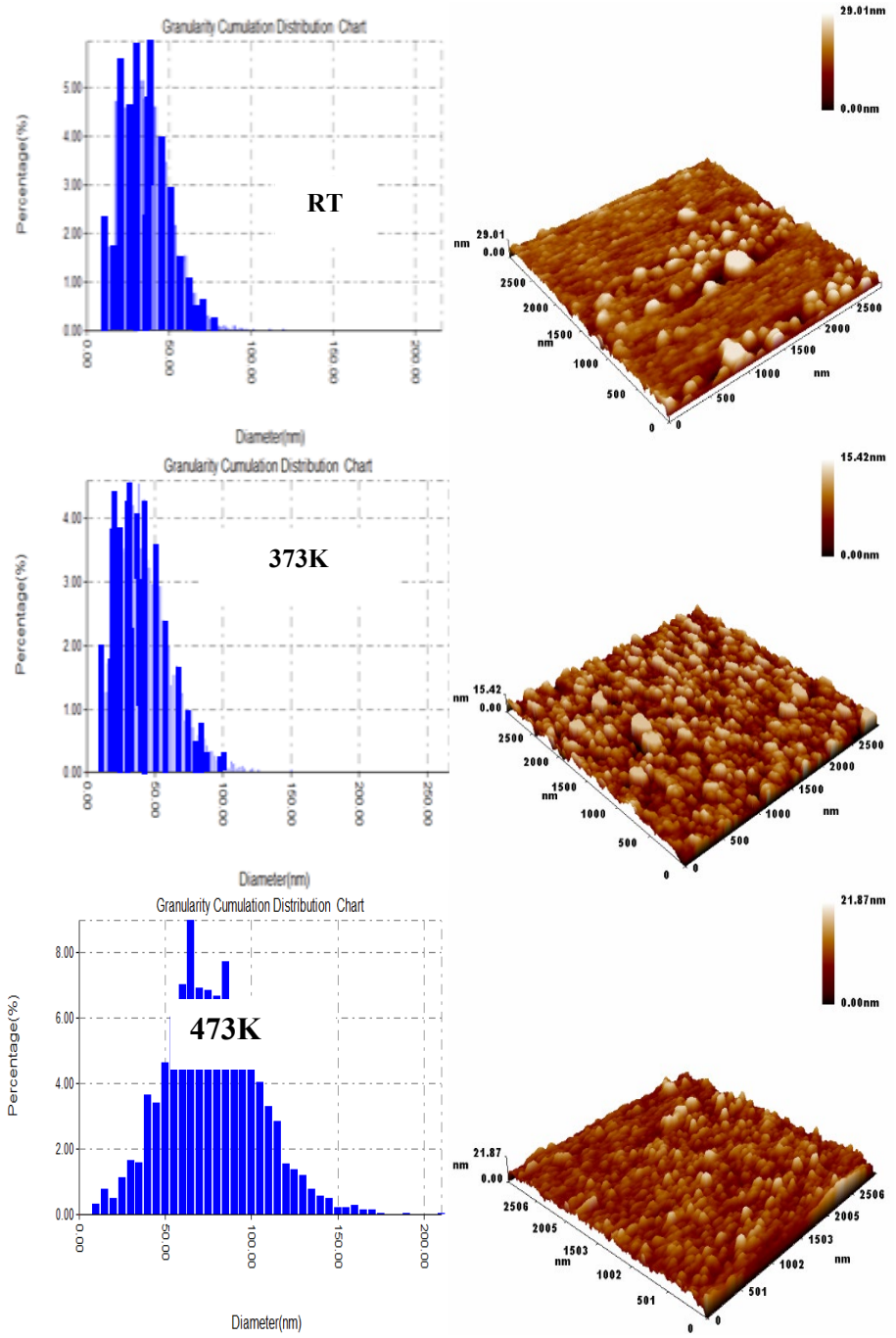

Fig. 2. A chart depicting Granularity, Cumulation, and Distribution, as well as three-dimensional visuals, was created for both as-deposited and annealed ZnTe films.

By examining the optical characteristics of ZnTe/glass at (373, 473) K, both as deposited and annealed, we have generated transmittance and absorbance spectra for ZnTe thin films with a wavelength range of (400-1000) nm. Figure (3) displays these spectra, which show a decrease in absorbance for all samples as the wavelength increases while increased in transmittance values and decrease transmittance value when increases of vacuum annealing temperatures. The high value of transmittance which means this good layer for window Materials for multi-layer solar cells as in report [8,35].

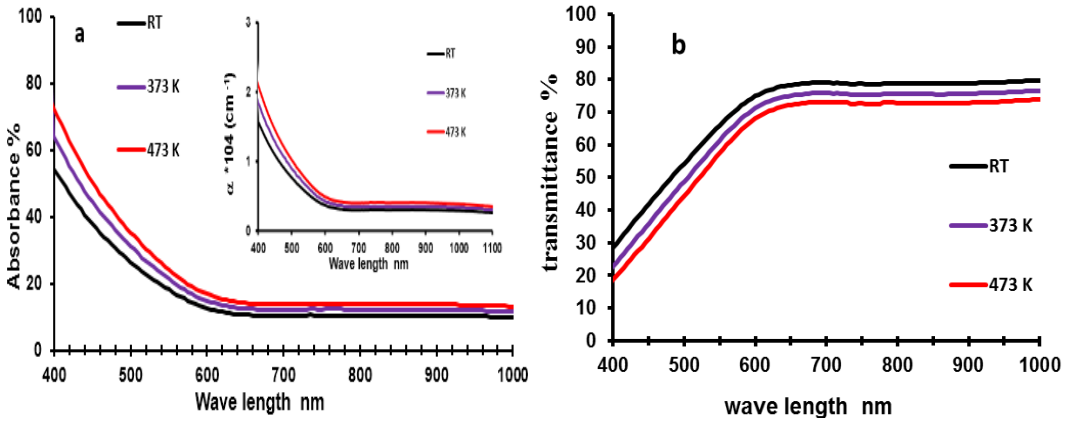

Fig. 3. (a) The Absorbance and (b)Transmittance spectrum with wavelength Inset: Absorption Coefficient for as deposited and annealed ZnTe film.

The absorption coefficient of ZnTe/glass films was calculated with the Urbach law. At strong absorption regions where absorption coefficient $\alpha > 10^4$ cm^{-1}. The allowed optical energy band gap of annealed ZnTe can be calculated by the Tauc equation. since the annealed ZnTe films are polycrystalline, as shown by X-ray diffraction, the transition will most likely be permissible that is mean transition is direct [34]. This can be done by extrapolation to zero the horizontal axis hυ in the Tauc equation. Figure 4 illustrates the variation of Eg for ZnTe thin films at room temperature and temperatures of 373 K and 473 K. The results show a reduction in the value of ZnTe/glass films as the annealing of the ZnTe layer increases. The optical energy gaps of the ZnTe films were calculated to be within the range of 2.3 eV to 2.2 eV, which are close to the reported values [7,10,12].

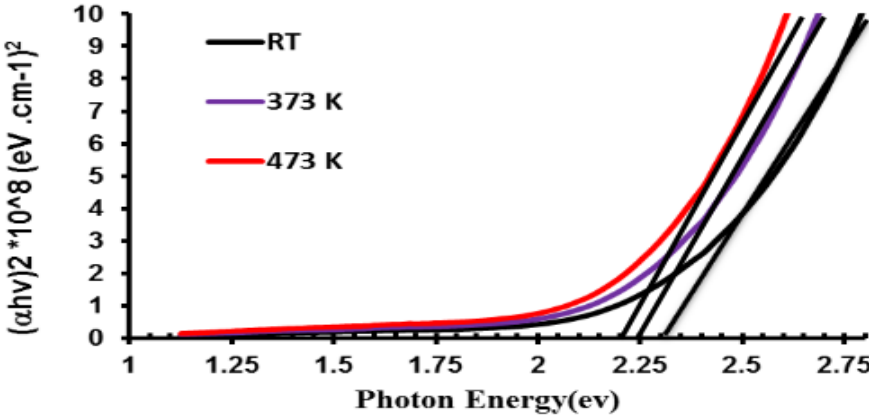

Fig. 4. The photon energy (Eg) for as-deposited and annealed ZnTe films was measured using $(\alpha h\upsilon)^2$.

Table 3. Optical parameter (E_g^{opt}, α, k, n, εr and εi) for as deposited and annealed ZnTe film thin where λ=400nm.

Thickness (100nm)	E_g^{opt} (eV)	$\alpha \times 10^4$ cm^{-1}	n	k	εr	εi	tan δ	δ*10^12
R.T	2.3	1.56	1.7	0.049	2.89	0.169	0.0587	6.28
473	2.25	1.8	1.56	0.058	2.44	0.182	0.075	6.8
573	2.2	2.1	1.42	0.067	2	0.188	0.094	7.0

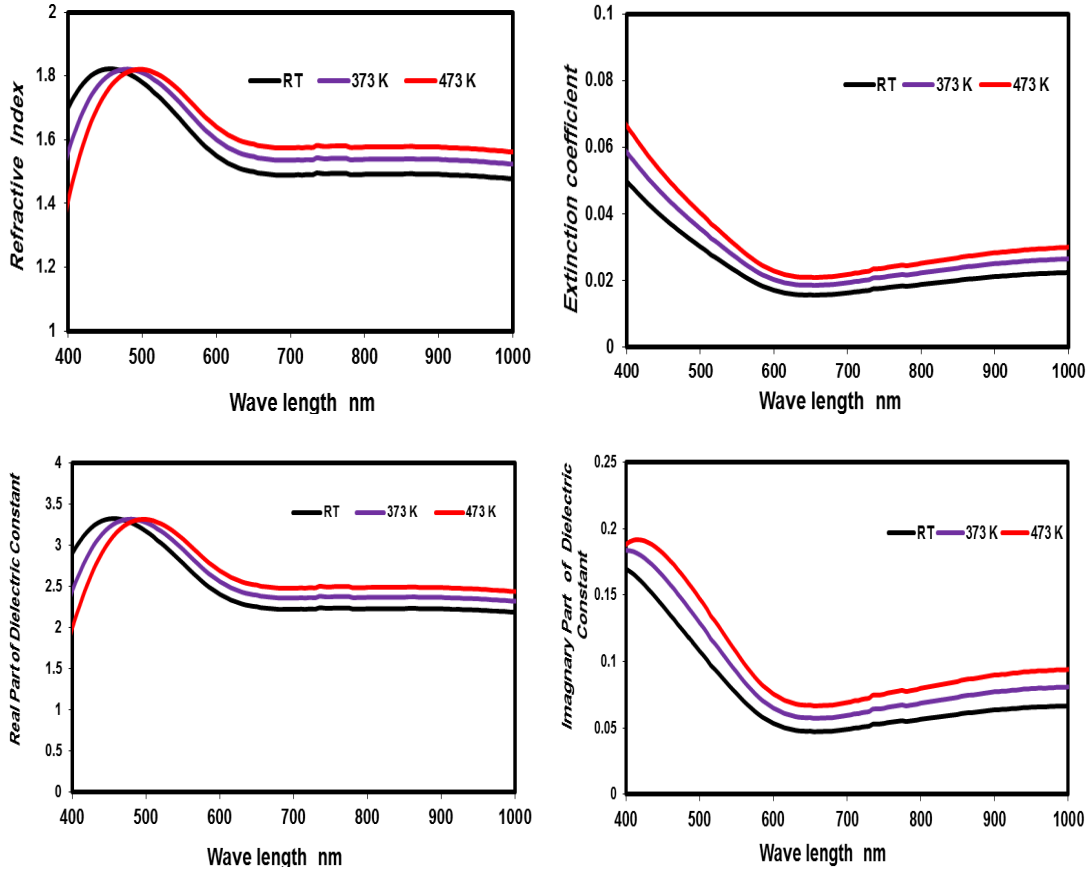

Fig. 5. The changes in refractive index, extinction coefficient, and the real and imaginary components of the dielectric constant as a function of wavelength were analyzed for ZnTe films in both as-deposited and annealed states.

The parameters related to optics, commonly referred to as optical constants, hold significant importance in optical materials and their various applications (Table 3) is provided below, which enlists the computed values of optical constants at a wavelength (λ) of 400nm.The refractive index (n) and the extinction coefficient (k) calculated from reflectivity and absorption spectra respectively of ZnTe thin film as in Figure 5. After λ =500nm it was saw that the refractive index increased with the increase of the heat-treated of the ZnTe film. which was attributed to the rise in crystallites size (XRD) and grain size (AFM) which led to the rise in crystallinity of crystal, [36]. With vacuum annealing, the corresponding reflection decreases, leading to a decrease in the values of n. this result agrees with the good values of refractive index make ZnTe film more suitable for antireflection multilayer. While the the extinction coefficient (k) increased with vacuum annealing attributable to increasing of absorption The complex dielectric constant is contain of and the real and imaginary part of the dielectric constant for ZTe thin film. The value of the real part (εr) is related to the ability of materials to slow down the speed of light [33]. When compared to εi, εr has a larger value due to n >>> k. Figure 6 illustrates the difference in the dielectric loss function for ZnTe thin film, which indicates a decrease in the function with an increase in wavelength, and a maximum value of 0.094 at a wavelength of 400 nm. The optical conductivity of ZnTe thin films also decreases as the wavelength increases and high value in $7*10^{12}$.

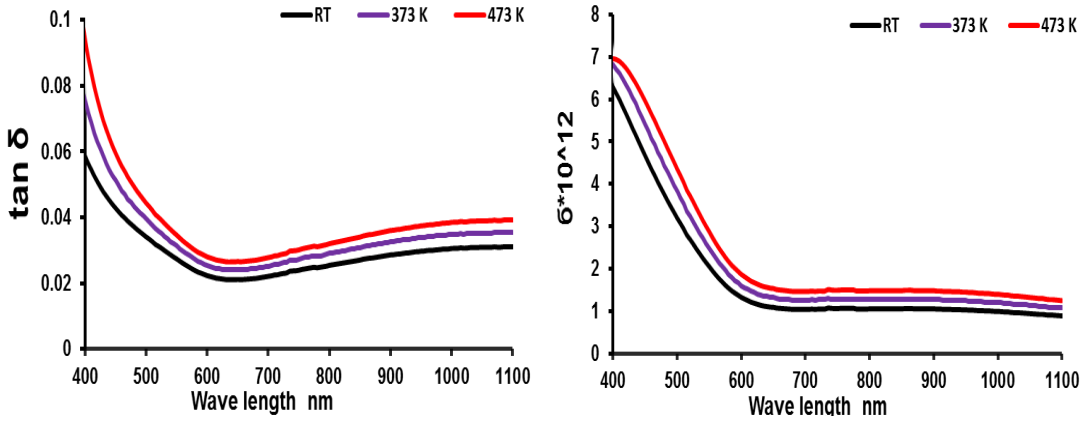

Fig. 6. Variation of dielectric loss function and optical conductivity for as deposited and annealed ZnTe films.

To find the film type (n or p), carrier concentrations, mobility and resistivity of ZnTe films thin, it should estimate the Hall effect as show in the Table (4), it can see the electrical resistivity of ZnTe films thin at heat-treated is lower than that of the R.T thin film. The positive sign of the $R_{(H)}$ shows that the conductivity of all the grown films are p-type behavior, similar behaves was obtained in [24,27]. The carrier concentrations was $10^{13}cm^{-3}$ orders, that good contract with the research [24,37,38]. It can notice from Table 4 and Figure 7, The sample at vacuum annealing temperatures 473 K is considered to be the best among all the samples because it has a high bulk carrier concentration (3.99×10^{13} cm^{-3}), high hole mobility (407.26 cm2/Vs) that the mobility and concentration rises after at heat-treated this designate that the development in the film structure and decrease grain boundary scattering.

Table 4. Hall parameters of for as deposited and annealed ZnTe films thin.

Thickness(100 nm)	$R_{(H)}$	p (cm^{-3})*10^{13}	$\mu_H(cm^2/V.S)$
R.T	281531.5	2.22	337.8378
373	175070	3.57	350.1401
473	156641.6	3.99	407.2682

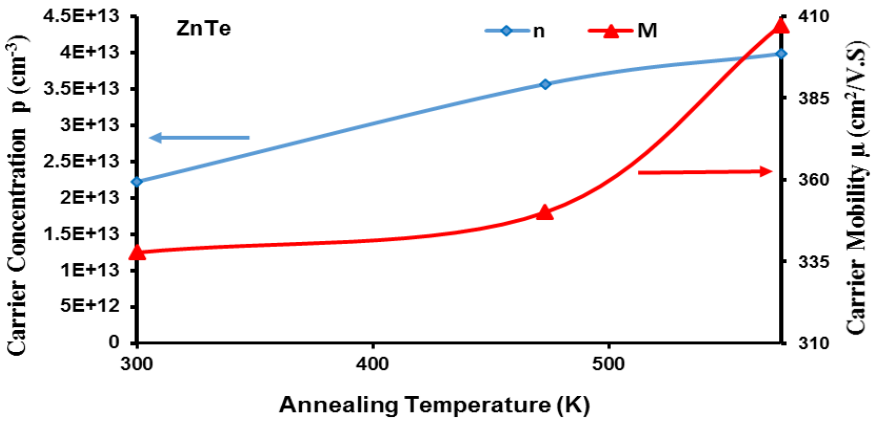

Fig. 7. Hall parameters of for as deposited and annealed ZnTe films.

4. Conclusions

It is possible to manufacture ZnTe thin films at R.T and heat-treated elevated temperatures by vacuum evaporation considered is a simple and suitable method for depositing very good quality ZnTe thin film. The ZnTe layers deposited with bandgap values lies between 2.3-2.2 eV. ZnTe layers has a polycrystalline cubic structure, a preferential orientation in the 111 direction with crystallite size 16.7 nm at 473 K. Hall effect measurement show that the properties of ZnTe samples p-type depend on vacuum annealing temperatures. The ZnTe film have 80 % light is transmitted so can be used as a window layer for solar cells.

References

[1] F Fauzi, D G Diso, O K Echendu, V Patel, Y Purandare, R Burton and I M Dharmadasa, Semiconductor Science and Technology, 28(4),(2013), 045005; https://doi.org/10.1088/0268-1242/28/4/045005

[2] BushraK H AlMaiyaly, Bushra H Hussein Auday H Shaban , IOP Conf. Series: Journal of Physics: (2018) 1003; https://doi.org/10.1088/1742-6596/1003/1/012084

[3] T. Mahalingam, V.S. John, S. Rajendran and P.J. Sebastian, Semiconductor Science and Technology. 17 (5) (2002) 465; https://doi.org/10.1088/0268-1242/17/5/310

[4] M. Neumann-Spallart and C. Koenigstein, Thin Solid Films. 265, 33, (1995); https://doi.org/10.1016/0040-6090(95)06641-1

[5] Dumitru Manica, Vlad-Andrei Antohe , Antoniu Moldovan, Rovena Pascu, Sorina Iftimie, Lucian Ion, Mirela Petruta Suchea and Stefan Antohe, nanomaterials, 11, 2286 (2021); https://doi.org/10.3390/nano11092286

[6] Suthar, D.; Himanshu; Patel, S.L.; Chander, S.; Kannan, M.D.; Dhaka, M.S., Solid State Sci., 107, 106346 (2020); https://doi.org/10.1016/j.solidstatesciences.2020.106346

[7] Samir A. Maki, Hanan K. Hassun, Ibn Al-Haitham J. for Pure & Appl. Sci. Vol.29 (2) (2016).

[8] A.B.M.O. Islam, N.B. Chaure, J. Wellings, G. Tolan, I.M. Dharmadasa, Mater. Charact, 60, (2009) 160 – 163; https://doi.org/10.1016/j.matchar.2008.07.009

[9] Sharma,D. C.; Srivastava ,S.; Vijay1, Y.K. and Sharma, Y.K. Effect of Mn-Doping on Optical Properties of ZnTe Thin Films, International Journal of Recent Research and Review (2012); https://doi.org/10.1063/1.3606080

[10] Bushra H. Hussein, Hanan K. Hassun, NeuroQuantology, 18(5) (2020) 77-82; https://doi.org/10.14704/nq.2020.18.5.NQ20171

[11] Kim T, Kim Y, Lee I, LeeDand Sohn H Ovonic threshold switching in polycrystalline zinc telluride thin films deposited by RF sputtering Nanotechnology 30, 13, (2019); https://doi.org/10.1088/1361-6528/aafe13

[12] R Zarei,M H Ehsani and H Rezaghiolipour Dizaji, Mater. Res. Express 7 026419 (2020); https://doi.org/10.1088/2053-1591/ab7691

[13] Ur Rehman, Khalid Mehmood ;Liu, Xiansong ;Riaz, Muhammad ;Yang, Yujie ; Feng, Shuangjiu ; Khan,Muhammad Wasim ; Ahmad, Ashfaq ;Shezad, Mudssir ;Wazir, Z. ; Ali, Zulfiqar ; Batoo, Khalid Mujasam ; Adil, Syed Farooq ; Khan, Mujaeeb ; Raslan, Emad H., Physica B 560 204-207 (2019); https://doi.org/10.1016/j.physb.2019.02.043

[14] Harinder Singh, Tejbir Singh, Anup Thakur and Jeewan Sharma, International journal of Research in Science and Engineering, 7 (8) (2018).

[15] Olusola O I, Madugu M L, Abdul-Manaf N A and Dharmadasa I M, Curr. Appl. Phys. 16 120-30 (2016); https://doi.org/10.1016/j.cap.2015.11.008

[16] He S, Lu H, Li B, Zhang J, Zeng G,WuL, Li W, WangWand Feng L, Sci. Semicond. Proess 67 41-5 (2017); https://doi.org/10.1016/j.mssp.2017.05.009

[17] Nakasu T, Sun W, KobayashiMand Asahi T, J. Cryst. Growth. 468 635-7 (2017); https://doi.org/10.1016/j.jcrysgro.2016.11.035

[18] Tanaka T, Ohshita H, SaitoKand GuoQ, Superlattices. Microstruct 114 192-919 (2018); https://doi.org/10.1016/j.spmi.2017.12.034

[19] Mondal A, Chaudhuri S and Pal AK, Appl. Phys. A 43 81-4 (1987); https://doi.org/10.1007/BF00615211

[20] Isik M, Gullu H H, Parlak M and Gasanly N M, Phys B 582 411968-73 (2020); https://doi.org/10.1016/j.physb.2019.411968

[21] Sachin D.Kshirsagar , M.GhanashyamKrishna, SuryaP.Tewari, Materials Science in Semiconductor Processing 16 1002-1007 (2013); https://doi.org/10.1016/j.mssp.2013.02.015

[22] Mohammed S.Mohammed, Eng.&Tech.26 (6) ,(2008).

[23] Murilo F. Gromboni, Francisco W. S. Lucas and Lucia H. Mascaro, J. Braz. Chem. Soc., 25,(3), (2014) 526-531.

[24] M. Abbas N. A. Shah, K. Jehangir, M. Fareed, A. Zaidi, Materials Science-Poland, 36(3), , (2018) 364-369; https://doi.org/10.1515/msp-2018-0036

[25] Iman Ahmed Younus, Anwar M. Ezzat and Mohammad M. Uonis, Nanocomposites,6, (4) (2020), 165-172; https://doi.org/10.1080/20550324.2020.1865712

[26] Wang, J. ; Isshiki, M., Wide-bandgap II-VI semiconductors: growth and properties. In Springer handbook of electronic and photonic materials, Springer. (2006) 325-342; https://doi.org/10.1007/978-0-387-29185-7_16

[27] Sarmad M. Ali, Alia A. A. Shehab and Samir A. Maki, Ibn Al-Haitham Jour. for Pure & Appl. Sci., Vol. 31 (3) (2018); https://doi.org/10.30526/31.3.2023

[28] R. H. Athab, B. H. Hussein, Digest Journal of Nanomaterials and Biostructures, 17 (4), (2023) 1173-1180; https://doi.org/10.15251/DJNB.2022.174.1173

[29] Chander, A. Purohit, C. Lal, and M.S. Dhaka, Mater. Chem. Phys. 185, (2017) , 202-209; https://doi.org/10.1016/j.matchemphys.2016.10.024

[30] S. N. Sobhi, B. H. Hussein, Chalcogenide Letters, 19(6) (2022) 409-416; https://doi.org/10.15251/CL.2022.196.409

[31] R. H. Athab, B. H. Hussein, Chalcogenide Letters, 20 (2), (2023) 91-100; https://doi.org/10.15251/CL.2023.202.91

[32] T. Mahalingam, V. Dhanasekaran, K. Sundaram, A. Kathalingam and J.-K. Rhee, Ionics, 18, (2012) 299-306; https://doi.org/10.1007/s11581-011-0623-6

[33] J. Li, D. R. Diercks, T. R. Ohno, C. W. Warren, M. C. Lonergan, J. D. Beach, C. A. Wolden, Sol. Energy Mater. Sol. Cells 133 (2015) 208-215; https://doi.org/10.1016/j.solmat.2014.10.045

[34] M. A. Sebaka,S. Ghalab, Atef El-Taher, E. R. Shaaban, Chalcogenide Letters 19(6) (2022) 389-408; https://doi.org/10.15251/CL.2022.196.389

[35] Sheikh Rashel Al Ahmed, Jannatul Ferdous, Md. Suruz Mian, IOP SciNotes, 1(2), (2020).

[36] T. Bellunato, M. Calvi, C. Matteuzzi, M. Musy, D. L. Perego, B. Storaci, Europ. Phys. J. 52 (2007) 759; https://doi.org/10.1140/epjc/s10052-007-0431-3

[37] Rana Hameed Athab, Bushra H. Hussein, Ibn Al-Haitham Journal for Pure and Applied Sciences, 35(4)2022; https://doi.org/10.30526/35.4.2868

[38] Bushra H. Hussein, Iman Hameed Khudayer, Mohammed Hamid Mustafa, Auday H. Shaban, An International Journal (PIE) 13(2), 173 (2019); https://doi.org/10.1504/PIE.2019.099358